

Review of H1 results on the hadronic final state at HERA

Lidia GOERLICH^{*†}

Institute of Nuclear Physics PAN, Cracow

E-mail: Lidia.Goerlich@ifj.edu.pl

The production of forward jets as well as charged particles in deep-inelastic positron-proton scattering at low photon virtuality Q^2 is measured with the H1 detector at HERA.

For inclusive DIS events with a forward jet, produced close to the proton remnant, differential cross sections and normalised distributions are measured in the laboratory frame as a function of the azimuthal angle difference, $\Delta\phi$, between the forward jet and the scattered positron in bins of the rapidity distance, Y , between them.

The analysis of charged particle production is performed in the hadronic centre-of-mass frame. The charged particle densities are measured as a function of pseudorapidity (η^*) and transverse momentum (P_T^*) in the range $0 < \eta^* < 5$ and $0 < P_T^* < 10$ GeV.

The data are compared to predictions of next-to-leading order QCD calculations and leading order Monte Carlo generators with different parton evolution approaches and with different hadronisation schemes.

The European Physical Society Conference on High Energy Physics -EPS-HEP2013

18-24 July 2013

Stockholm, Sweden

^{*}Speaker.

[†]On behalf of the H1 Collaboration.

1. Introduction

The HERA ep collider has extended the available kinematic range for deep-inelastic scattering (DIS) to regions of the Bjorken scaling variable, x , as small as 10^{-5} at moderate values of photon virtualities Q^2 of a few GeV^2 . At low x a parton in the proton can induce a QCD cascade before an interaction with the virtual photon. Several perturbative QCD-based approaches are available to describe the dynamics of the parton evolution process. In the standard DGLAP evolution [1] partons emitted in the cascade are strongly ordered in transverse momentum, P_T , measured with respect to the proton direction. At small values of x a transition is expected from DGLAP to BFKL dynamics [2] in which there is no ordering in P_T of the partons along the ladder. The CCFM [3] evolution aims to unify the DGLAP and BFKL approaches. It introduces angular ordering of gluon emissions to implement coherence effects.

Hadronic final state observables are sensitive to the dynamics of QCD processes and are thus expected to discriminate between different evolution approximations. To search for deviations from the P_T ordering measurements of DIS events with energetic jets of high transverse momentum produced close to the proton direction in the laboratory frame, referred to as the forward region, have been performed. The distribution of the azimuthal angle difference, $\Delta\phi$, between the forward jet and the scattered electron may show sensitivity to the underlying physics in the evolution of the parton cascade [4]. In this talk the study of the H1 Collaboration on the azimuthal correlation between the forward jet and the scattered positron in DIS at low x is presented [5].

Studies of the transverse momentum spectrum of charged particles have been proposed [6] as a more direct probe of the underlying parton dynamics. The high transverse momentum region is expected to be sensitive to parton evolution effects, while at low P_T hadronisation is expected to be more relevant. The charged particle densities measured in the hadronic centre-of-mass system as a function of pseudorapidity (η^*) and transverse momentum (P_T^*) are presented [7].

2. QCD calculations

The measurements presented are compared with predictions of Monte Carlo (MC) generators which implement various QCD models. RAPGAP [8] matches first order QCD matrix elements to DGLAP based leading-log parton showers with P_T ordering. The factorisation and renormalisation scales are set to $\mu_f = \mu_r = \sqrt{Q^2 + p_T^2}$, where p_T is the transverse momentum of the two outgoing hard partons in the centre-of-mass of the hard subsystem. DJANGO/ARIADNE is an implementation of the Colour Dipole Model (CDM) [9] in which the parton emissions perform a random walk in P_T such that CDM provides a BFKL-like approach. CASCADE [10] uses off-shell QCD matrix elements, supplemented with gluon emissions based on the CCFM evolution equation [3]. In these analyses two different sets of unintegrated gluon density (uPDF) are used (see [10]): set A0 with only singular terms of the gluon splitting function and J2003-set 2 including also non-singular terms. The Herwig++ [11] MC program combines the full matrix element including virtual corrections at $O(\alpha_S)$ with a DGLAP-like parton shower simulation. Here the parton branching is based on colour coherence to suppress branchings outside an angular-ordered region of phase space. For the hadronisation, the Lund string fragmentation [12] is used, as implemented in JETSET [13] for DJANHO/ARIADNE and in PYTHIA [14] for RARAPGAP and

CASCADE. In the study of charged particle production three sets of fragmentation parameters are compared to the data: parameters tuned by ALEPH [15], by the Professor tuning tool [16] and default PTYHIA6.624 fragmentation parameters. Herwig++ incorporates the cluster model [17] of hadronisation. In the forward jet analysis the data are also compared to the fixed order NLO DGLAP predictions of the NLOJET++ program [18].

3. Forward jet azimuthal correlations

The analysis phase space is restricted in Q^2 , x and inelasticity y : $5 < Q^2 < 85 \text{ GeV}^2$, $0.0001 < x < 0.004$, $0.1 < y < 0.7$. Events with at least one forward jet satisfying the following cuts in the laboratory frame are selected: $P_{T,\text{fwdjet}} > 6 \text{ GeV}$, $1.73 < \eta_{\text{fwdjet}} < 2.79$, $x_{\text{fwdjet}} = E_{\text{fwdjet}}/E_p > 0.035$ and $0.5 < P_{T,\text{fwdjet}}^2/Q^2 < 6$. Here η_{fwdjet} is the pseudorapidity of the forward jet. The last two cuts aim to enhance the effects of BFKL dynamics and suppress the DGLAP evolution.

The forward jet cross section $d\sigma/d\Delta\phi$ as a function of the azimuthal angle difference $\Delta\phi$ be-

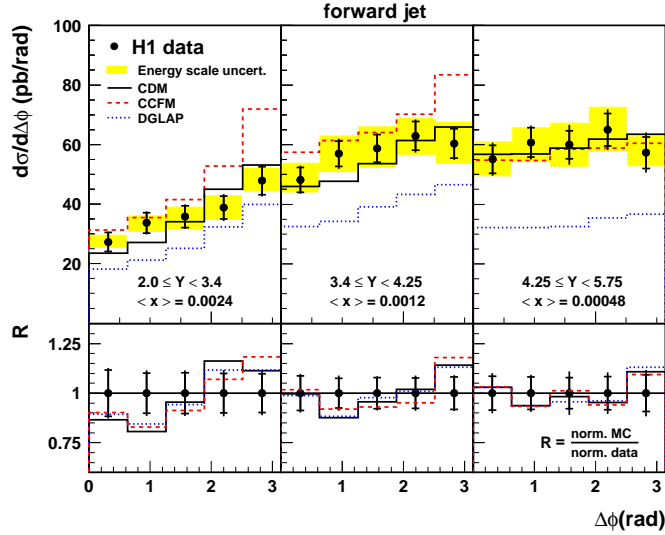


Figure 1: Differential forward jet cross section as a function of $\Delta\phi$ in three intervals of Y compared with the predictions of different QCD-based models. The systematic error due to the uncertainty of the hadronic energy scale is shown by the shaded band.

tween the most forward jet and the scattered positron is shown in Figure 1 for three intervals of the positron-jet rapidity distance Y . At higher values of Y the forward jet is decorrelated from the scattered positron. The predictions of three QCD-based models with different underlying parton dynamics are compared with the data. The cross sections are well described in shape and normalisation by the BFKL-like CDM model. Predictions of RAPGAP, labeled DGLAP, fall below the data, particularly at large Y . Calculations in the CCFM scheme as implemented in CASCADE, using the uPDF set A0 with only singular terms of the gluon splitting function, overestimate the measured cross section for large $\Delta\phi$ values in the two lowest Y intervals. However, this model provides as good a description as CDM of the data in the highest Y interval. The ratio R of MC to data for normalised cross sections shows that the shape of the $\Delta\phi$ distributions is described equally

well by all MC models and cannot discriminate between different QCD dynamics.

Predictions of the CCFM model shown in Figure 2 indicate a significant sensitivity to the choice

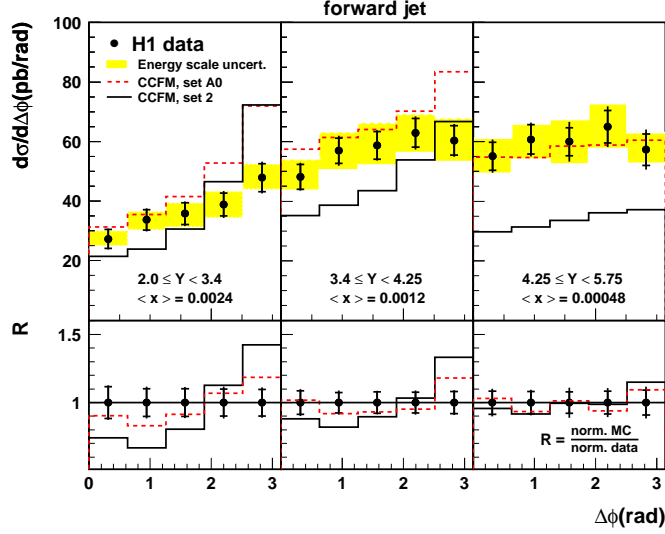


Figure 2: Differential forward jet cross section as a function of $\Delta\phi$ in three intervals of Y compared to the predictions of CASCADE(CCFM) with two different uPDF.

of the uPDF. The set A0 is the same as in Figure 1. Predictions using J2003-set 2, marked set 2, do not describe the data in normalisation especially at high Y and in shape especially at low Y .

DGLAP predictions at $O(\alpha_s^2)$ accuracy of the NLOJET++ program presented in Figure 3 are in general below the data, but still in agreement within the large theoretical uncertainties indicating that in this phase space region higher order contributions are expected to be important.

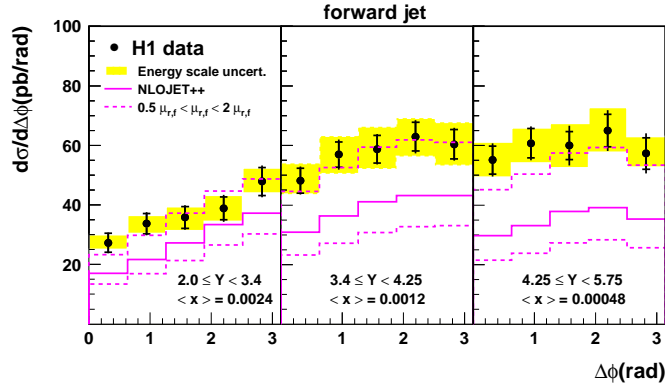


Figure 3: Differential forward jet cross section as a function of $\Delta\phi$ compared to NLO QCD predictions.

4. Charged particle production

The kinematic range of the analysis covers $5 < Q^2 < 100 \text{ GeV}^2$, $0.0001 < x < 0.01$ and $0.05 < y < 0.6$. The study is performed in the virtual photon-proton rest frame, the positive z^* axis is

defined by the direction of the virtual photon. The charged particle densities as a function of η^* measured separately for $P_T^* < 1$ GeV and for $1 < P_T^* < 10$ GeV are presented in Figure 4.

In the soft P_T^* region, the density of particles is almost flat for $1 < \eta^* < 3.5$. In the hard P_T^*

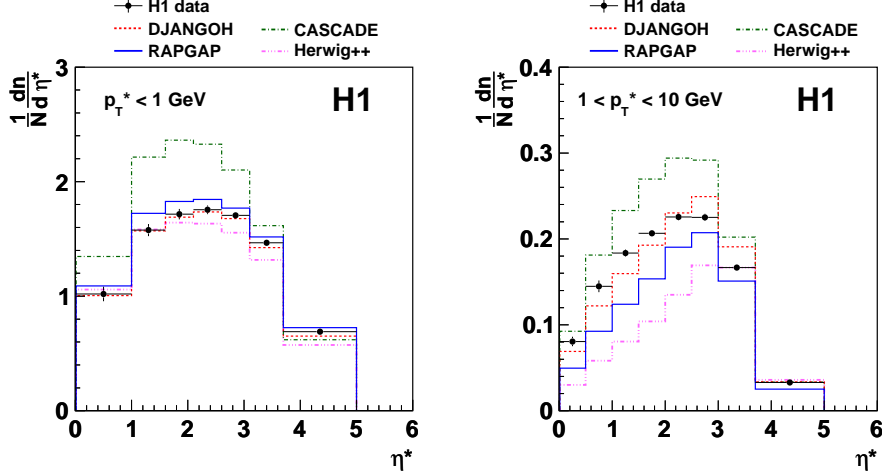


Figure 4: Charged particle density as a function of η^* for $P_T^* < 1$ GeV (left plot) and for $1 < P_T^* < 10$ GeV (right plot) compared with predictions of different QCD-based models.

region the density increases with increasing η^* up to $\eta^* \approx 2.5$ GeV, a behaviour expected from the strong ordering of transverse momentum towards the hard scattering vertex. The predictions of four models with different approaches for QCD radiation are compared to the data. At small P_T^* , the data are reasonably well described by DJANGO based on the CDM model, as well as the DGLAP-based MC RAPGAP and Herwig++. CASCADE predicts too high multiplicities in most of the measured η^* range. At high P_T^* , the strong sensitivity to the QCD dynamics is observed. DJANGO provides the best description of the data. RAPGAP and Herwig++ strongly undershoot the measurements, while CASCADE is significantly above the data.

To check the sensitivity to hadronisation effects, the RAPGAP predictions for three different sets of fragmentation parameters are compared to the data in Figure 5. At low P_T^* significant differences between these three samples are seen and the data are best described by the ALEPH tune. At large P_T^* they give similar results but none of them describes the data.

In Figure 6 the charged particle densities as a function of P_T^* are shown for two pseudorapidity intervals, $0 < \eta^* < 1.5$ and $1.5 < \eta^* < 5.0$, referred to as the “central region” and “current region”, respectively. Such division approximately defines the regions where the sensitivity to the hard scatter is large (current region), and where the effects of parton shower dynamics can be tested (central region). The proton target region, $\eta^* < 0$, is not accessible in this analysis.

The shapes of the measured P_T^* distributions in the two pseudorapidity ranges are similar. The predictions of four QCD-based models with different underlying parton dynamics are compared with the data. DJANGO provides a reasonable description of the data, only at high P_T^* in the current region deviations from the measurement are observed. The other models fail to describe the data, with the strongest deviations being observed in the central region.

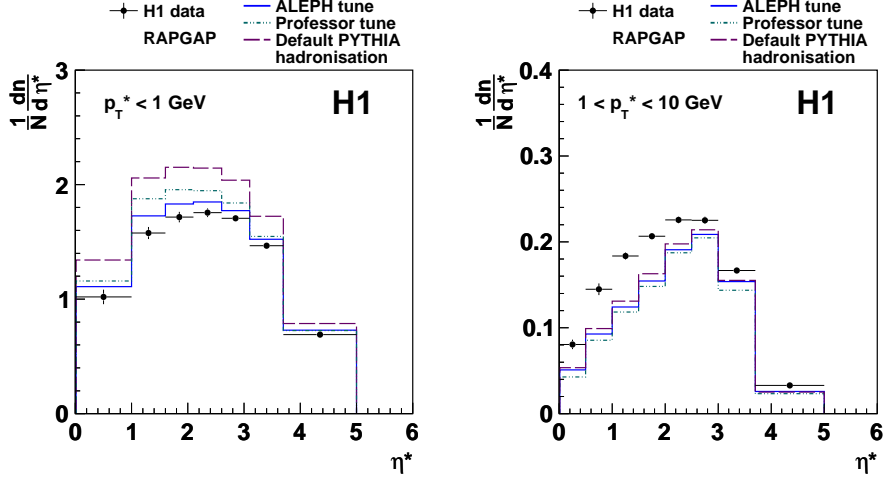


Figure 5: Charged particle density as a function of η^* for $P_T^* < 1$ GeV (left plot) and for $1 < P_T^* < 10$ GeV (right plot) compared to RAGAP predictions for three different sets of fragmentation parameters.

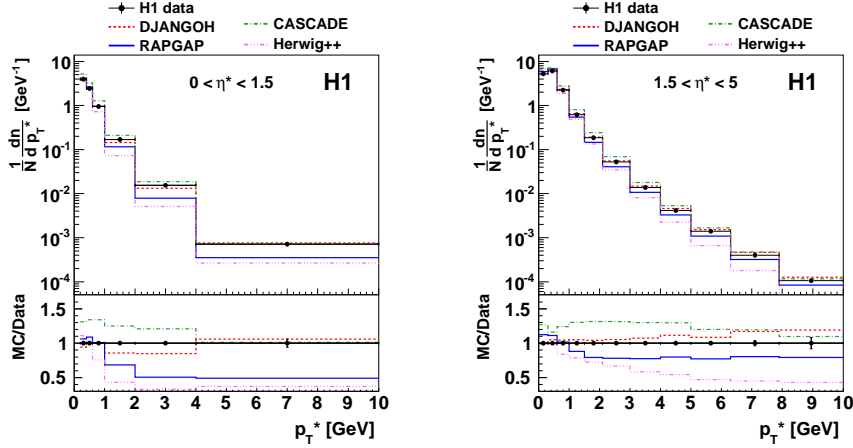


Figure 6: Charged particle density as a function of P_T^* in the ranges $0 < \eta^* < 1.5$ (left plot) and $1.5 < \eta^* < 5.0$ (right plot) compared with predictions of different QCD-based models.

5. Conclusions

Recent measurements of the hadronic final states in DIS at low Q^2 sensitive to the dynamics of parton evolution as well as to different hadronisation schemes performed by the H1 Collaboration were discussed. They include the study of the azimuthal correlation in the production of forward jets, produced close to the proton direction, and also investigations of the charged particle densities as a function of pseudorapidity and transverse momentum.

Differential forward jet cross sections and normalised distributions are measured in the laboratory frame as a function of the azimuthal angle difference between the forward jet and the scattered positron for different regions of the rapidity separation between them. The cross sections are best described by the BFKL-like Colour Dipole Model, while the DGLAP-based RAGAP model is

substantially below the data. The CCFM-based CASCADE predictions depend strongly on the un-integrated gluon density. The shapes of the $\Delta\phi$ distributions are equally well described by leading order Monte Carlo models with different QCD evolution schemes. The fixed order NLO DGLAP predictions are in general below the data, but still in agreement within the large theoretical uncertainties.

The transverse momentum and pseudorapidity distributions of the charged particles are measured in the hadronic centre-of-mass system. The data are compared to QCD-based models with different parton evolution dynamics and with different hadronisation schemes. The P_T -ordered parton shower modelled by RAPGAP as well as Herwig++, which also uses the cluster fragmentation model, are below the data especially at high P_T^* and low η^* . The CCFM-based CASCADE predicts in most regions of phase space higher particle densities than observed in the data. The CDM model is the best among the considered models and provides a reasonable description of the data.

References

- [1] G. Altarelli and G. Parisi, *Nucl. Phys.* **B126** (1977) 298.
- [2] E. Kuraev, L. Lipatov and V. Fadin, *Sov. Phys. JETP* **45** (1977) 199.
- [3] S. Catani, F. Fiorani and G. Marchesini, *Nucl. Phys.* **B336** (1990) 18.
- [4] J. Bartels *et al.*, *Phys. Lett.* **B384** (1996) 300 [hep-ph/9604345].
- [5] F. D. Aaron *et al.*, [H1 Collaboration], *Eur. Phys. J.* **C72** (2012) 1910 [arXiv:1111.4227].
- [6] M. Kuhlen, *Phys. Lett.* **B382** (1996) 441 [hep-ph/9606246].
- [7] C. Alexa *et al.*, [H1 Collaboration], *Eur. Phys. J.* **C73** (2013) 2406 [arXiv:1302.1321].
- [8] H. Jung, *Comput. Phys. Commun.* **86** (1995) 147.
- [9] L. Lönnblad, *Comput. Phys. Commun.* **71** (1992) 15.
- [10] H. Jung, *Comput. Phys. Commun.* **143** (2002) 100;
H. Jung, *et al.* CASCADE2.2.0, *Eur. Phys. J.* **C70** (2010) 1237.
- [11] S. Gieseke *et al.*, *Herwig++ 2.5* [arXiv:1102.1672].
- [12] B. Andersson *et al.*, *Phys. Rept.* **236** (1994) 227.
- [13] T. Sjöstrand *et al.*, *Comput. Phys. Commun.* **82** (1994) 174 [hep-ph/9508391].
- [14] T. Sjöstrand *et al.*, *Comput. Phys. Commun.* **135** (2001) 238 [hep-ph/0010017].
- [15] S. Schael *et al.*, [ALEPH Collaboration], *Phys. Lett.* **B606** (2005) 265.
- [16] A. Buckley *et al.*, *Eur. Phys. J.* **C65** (2010) 33 [arXiv:0907.2973].
- [17] B.R. Webber, *Nucl. Phys.* **B238** (1984) 492;
G. Marchesini and B.R. Webber, *Nucl. Phys.* **B310** (1988) 461.
- [18] Z. Nagy and Z. Trocsanyi, *Phys. Lett.* **87** (2001) 82001 [hep-ph/0104315].